A Mouse Model for Human Norovirus

Stefan Taube,[a]* Abimbola O. Kolawole,[a] Marina Höhne,[b] John E. Wilkinson,[c] Scott A. Handley,[d] Jeffrey W. Perry,[a] Larissa B. Thackray,[d] Ramesh Akkina,[e] Christiane E. Wobus[a]

Department of Microbiology and Immunology, University of Michigan, Ann Arbor, Michigan, USA[a]; Consultant Laboratory for Noroviruses, Robert Koch-Institute, Berlin, Germany[b]; Unit for Laboratory Animal Medicine and Department of Pathology, University of Michigan, Ann Arbor, Michigan, USA[c]; Department of Pathology and Immunology, Washington University, St. Louis, Missouri, USA[d]; Department of Microbiology, Immunology and Pathology, Colorado State University, Fort Collins, Colorado, USA[e]

* Present address: Stefan Taube, Institute for Virology and Cell Biology, University of Lübeck, Lübeck, Germany.

S.T. and A.O.K. contributed equally to this work.

ABSTRACT **Human noroviruses (HuNoVs) cause significant morbidity and mortality worldwide. However, despite substantial efforts, a small-animal model for HuNoV has not been described to date. Since "humanized" mice have been successfully used to study human-tropic pathogens in the past, we challenged BALB/c mice deficient in recombination activation gene (Rag) 1 or 2 and common gamma chain (γc) (Rag-γc) engrafted with human CD34$^+$ hematopoietic stem cells, nonengrafted siblings, and immunocompetent wild-type controls with pooled stool isolates from patients positive for HuNoV. Surprisingly, both humanized and nonhumanized BALB/c Rag-γc-deficient mice supported replication of a GII.4 strain of HuNoV, as indicated by increased viral loads over input. In contrast, immunocompetent wild-type BALB/c mice were not infected. An intraperitoneal route of infection and the BALB/c genetic background were important for facilitating a subclinical HuNoV infection of Rag-γc-deficient mice. Expression of structural and nonstructural proteins was detected in cells with macrophage-like morphology in the spleens and livers of BALB/c Rag-γc-deficient mice, confirming the ability of HuNoV to replicate in a mouse model. In summary, HuNoV replication in BALB/c Rag-γc-deficient mice is dependent on the immune-deficient status of the host but not on the presence of human immune cells and provides the first genetically manipulable small-animal model for studying HuNoV infection.**

IMPORTANCE **Human noroviruses are a significant cause of viral gastroenteritis worldwide, resulting in significant morbidity and mortality. Antivirals and vaccines are currently not available, in part due to the inability to study these viruses in a genetically manipulable, small-animal model. Herein, we report the first mouse model for human noroviruses. This model will accelerate our understanding of human norovirus biology and provide a useful resource for evaluating antiviral therapies.**

Received 18 June 2013 **Accepted** 20 June 2013 **Published** 16 July 2013

Citation Taube S, Kolawole AO, Höhne M, Wilkinson JE, Handley SA, Perry JW, Thackray LB, Akkina R, Wobus CE. 2013. A mouse model for human norovirus. mBio 4(4):e00450-13. doi:10.1128/mBio.00450-13.

Editor Terence Dermody, Vanderbilt University School of Medicine

Address correspondence to Christiane E. Wobus, cwobus@umich.edu, or Ramesh Akkina, ramesh.akkina@colostate.edu.

Human noroviruses (HuNoVs) are the leading etiologic agent of viral epidemic gastroenteritis globally in people of all ages (1), causing an estimated 200,000 deaths each year in children under 5 years old in developing countries (2). In the United States, ~21 million cases of gastroenteritis and ~800 deaths due to HuNoV occur annually, making HuNoV infections the leading cause of death among individuals with viral gastroenteritis (3, 4). Virus transmission occurs by the fecal-oral route, with person-to-person and food- or waterborne spread being the most common (5). The economic impact of these infections is staggering, with an economic cost for norovirus (NoV)-associated food-borne outbreaks alone of $5.8 billion annually in the United States (6). Unfortunately, no specific therapies are currently available to control or prevent HuNoV infections.

HuNoV research has been stifled by the absence of a HuNoV cell culture system and a genetically manipulable small-animal model for HuNoV. Some aspects of HuNoV biology have been studied in chimpanzees (7), gnotobiotic pigs, and calves (8, 9). However, these large-animal models are cumbersome, expensive, and not widely available.

HuNoVs are single-stranded positive-sense [(+)-sense] RNA viruses in the *Caliciviridae* family (10). Their ~7.5-kb genome encodes three open reading frames (ORFs). ORF1 encodes the nonstructural proteins N-terminal protein or NS1/2, NTPase or NS3, 3A-like protein or NS4, VPg (viral protein, genome-linked) or NS5, protease or NS6, and RNA-dependent RNA polymerase (RdRp) or NS7, while ORF2 and -3 encode the major and minor capsid proteins VP1 and VP2, respectively (10). HuNoVs are classified based on sequence similarity into three genogroups (GI, GII, and GIV) and at least 25 genotypes (11). However, the majority of HuNoV strains causing outbreaks today belong to the GII, genotype 4 (GII.4) cluster (12). Over the past decade, GII.4 epidemics

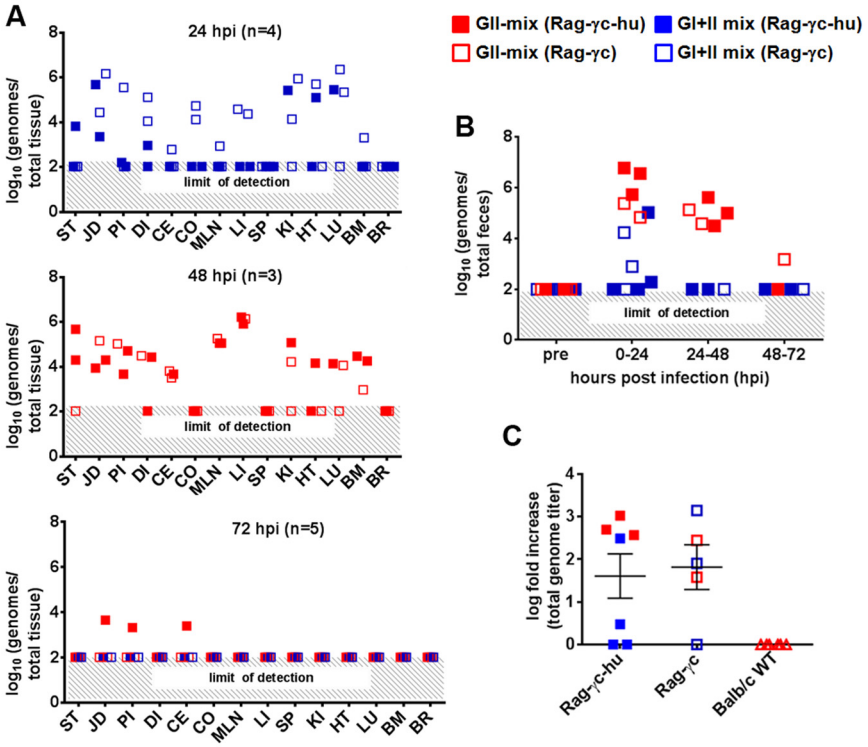

FIG 1 HuNoV infects humanized and nonhumanized Rag$^{-/-}$ γc$^{-/-}$ mice. Mice were infected intraperitoneally and orally with HuNoV-containing stool filtrates. Symbols indicate the mouse background: open, Rag-γc; filled, Rag-γc-hu. Open triangles indicate wild-type (wt) mice. Inocula are colored blue (GI+II mix) or red (GII mix). (A) HuNoV genomes were measured by qRT-PCR in stomach (ST), jejunum/duodenum (JD), proximal ileum (PI), distal ileum (DI), cecum (CE), and colon (CO), mesenteric lymph nodes (MLN), liver (LI), spleen (SP), kidney (KI), heart (HT), lung (LU), bone marrow (BM), and brain (BR) from mice sacrificed 24 (top panel), 48 (middle panel), or 72 (bottom panel) hours postinfection (hpi). (B) HuNoV genomes were measured in total feces excreted 12 h before infection (pre) or between 0 to 24, 24 to 48, or 48 to 72 hpi. (C) Total genome titers recovered from humanized (Rag-γc-hu), nonhumanized (Rag-γc), and wild-type (WT) BALB/c mice at the time of harvest were compared to inoculum titers to determine the log fold increase in viral titer over inoculum. Data are from at least two independent experiments, and each symbol represents titers from an individual mouse.

have occurred every 2 to 3 years, with new strains emerging by mutation and recombination (13), including the most recent GII.4 variant, Sydney 2012 (14).

To combat the problem of HuNoV morbidity and mortality, a widely accessible, genetically manipulable, small-animal platform and reproducible tissue culture system are urgently needed to investigate molecular mechanisms regulating HuNoV infection and to develop effective antiviral strategies (15). Here we report overcoming one of these major barriers in the field through the development of the first mouse model for HuNoV.

RESULTS

Reconstitution of a humanized immune system is not required for susceptibility of mice to HuNoV. HuNoV antigen is detected in B lymphocytes and dendritic cells in the intestinal lamina propria of HuNoV-infected chimpanzees (7), and a HuNoV GII.4 strain binds to cells in the lamina propria of human duodenum in an *in vitro* whole-virus binding assay (16). This raised the possibility that HuNoV may replicate in human immune cells. To test whether human immune cells are important for HuNoV infection, we used "humanized" mice (i.e., mice engrafted with human CD34$^+$ hematopoietic stem cells to reconstitute a functional human immune system) (35). Recombination activation gene (Rag) 1 or 2- and common γ-chain (γc)-deficient (Rag$^{-/-}$ γc$^{-/-}$) BALB/c mice were irradiated 2 to 3 days after birth and injected with human CD34$^+$ hematopoietic stem cells, as previously described (17). Approximately 6 months later, when these mice had reconstituted a human immune system, seven humanized mice, five nonhumanized Rag$^{-/-}$ γc$^{-/-}$ mice, and six BALB/c wild-type mice were challenged with pooled stool suspensions from patients containing either GI and GII (GI+II mix) or only GII (GII mix) HuNoV strains (see Table S1 in the supplemental material and Materials and Methods). Mice were infected with 8.56 × 10^3 GI and 4.08 × 10^3 − 7.08 × 10e4 GII total genomes (for GI+II mix) or 7.45 × 10^3 GII total genomes (for GII mix) (see Table S2 in the supplemental material).

Mice were initially challenged with pooled human stool samples by both the intraperitoneal and oral routes to increase the chance of detecting HuNoV replication (Fig. 1; see also Table S2 in the supplemental material). All tissue and fecal samples from the 12 humanized and nonhumanized mice were analyzed using multiplex quantitative reverse transcriptase PCR (qRT-PCR) as described elsewhere (18) to measure GI and GII genome loads. No GI sequences were detected in murine feces or tissues in any of the 7 mice infected with the GI+II mix for 24 or 72 h postinfection (hpi) (see Table S2 in the supplemental material). Therefore, only pooled human stool suspensions containing GII viruses (GII mix) were used for subsequent infections, in which mice were infected for 48 or 72 hpi. None of the mice succumbed to infection, but one humanized mouse with high titers in feces and tissue developed

watery diarrhea 24 hpi (mouse 3 in Table S2 in the supplemental material; also data not shown).

Analysis of the tissue samples indicated that HuNoV GII genomes were detectable in tissues from both humanized (5/7) and nonhumanized (4/5) mice (see Table S2 in the supplemental material). Tissue titers peaked at 24 to 48 hpi but declined by 72 hpi (Fig. 1A). HuNoV genomes were present in all regions of the intestine and in many of the extraintestinal sites (Fig. 1A; see also Table S2 in the supplemental material). The tissue sites consistently negative for HuNoV genome were brain and spleen. These data suggest that HuNoV does not cross the blood-brain barrier of humanized and nonhumanized mice.

Analysis of fecal samples indicated that GII genomes were detected in feces from 9 out of 12 mice, with similar proportions of humanized (5/7) and nonhumanized (4/5) mice (see Table S2 in the supplemental material). No HuNoV genomes were detected in murine feces prior to infection, but fecal titers peaked at 24 hpi (Fig. 1B). Of the 8 mice with detectable HuNoV genome titers in the tissues, only one had no detectable genome in the feces (see Table S2 in the supplemental material, mouse 8). In analogy to epidemiological analysis of HuNoV outbreaks (e.g., see reference 19), we obtained sequence information for HuNoV strains present in murine feces. Genotyping of murine feces revealed the presence of GII.4 genotype in feces from 8 out of 9 mice with detectable fecal titers. A natural recombinant, GII.g/II.1, was the only other genotype isolated from mouse feces. This GII strain exhibits closest sequence homology in the polymerase region to GII.g strains, while a region in the capsid aligned more closely with those of GII.1 strains. Interestingly, no GII.g/II.1 genomes were detected in the inoculum (see Table S1 in the supplemental material), suggesting that this genotype may have been present in human stool in quantities below the limit of detection. A GII.6 genotype that was detected in one of the human stools present in the GII mix (see Table S1 in the supplemental material) was not recovered from infected mice (see Table S2 in the supplemental material). Thus, the GII.4 isolate was detected predominantly in murine feces, possibly because it was present at higher titers than the other genotypes in the inoculum. Whether GI.3, GII.6, or other genotypes are infectious at higher doses or in general needs to be analyzed in the future to clarify the strain dependence in this model.

Since qRT-PCR for HuNoV does not distinguish between input and replication of HuNoV, genomes in tissues and murine feces at the experimental endpoint were combined and compared to the inoculum titer to determine whether HuNoV replicated in mice. Four of seven humanized and four of five nonhumanized animals showed 3- to 1,400-fold increases in genome titers over input (Fig. 1C; see also Table S2 in the supplemental material). This analysis suggested that HuNoV replicated in 9 of 12 mice following a combined intraperitoneal and oral challenge. No statistically significant difference using the Mann-Whitney U test ($P = 1.000$) was observed in the log fold increase between the humanized and nonhumanized mice challenged with HuNoV. Six BALB/c mice infected with the GII mix (1.47×10^5 GII genome copies total/mouse) intraperitoneally and orally showed no increases in genome loads over input (Fig. 1C). Taken together, these data suggest that HuNoV infection of Rag$^{-/-}$ $\gamma c^{-/-}$ mice can occur in the absence of human immune cells and show that the immunodeficiency conferred by the lack of Rag and/or γc is required for HuNoV replication in mice.

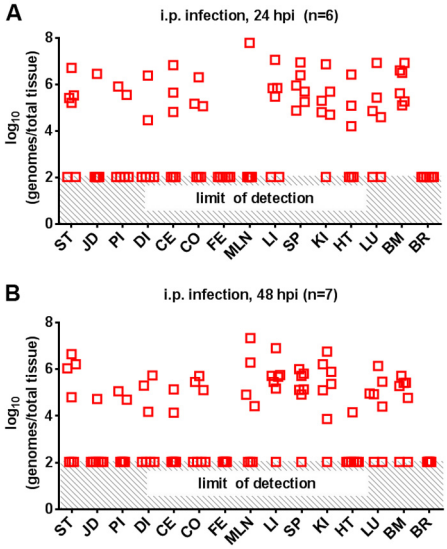

FIG 2 HuNoV infects Rag$^{-/-}$ $\gamma c^{-/-}$ mice by the intraperitoneal route. BALB/c Rag$^{-/-}$ $\gamma c^{-/-}$ mice were infected intraperitoneally with $1.11 \times 10e5 - 4.63 \times 10^6$ genomes of HuNoV GII mix for 24 (A) or 48 (B) hours. HuNoV genomes in tissues (abbreviations as in Fig. 1) were measured by qRT-PCR. Data are from four independent experiments, and each symbol represents titers from an individual sample.

Minimal changes occurred in the fecal GII.4 HuNoV sequence. Adaptation of human viruses is frequently required to establish robust infection in a mouse model (e.g., see reference 20). To determine whether HuNoV adapted to its murine host, we determined the complete sequence from an inoculating human stool sample (sample 9 [see Table S1 in the supplemental material]) (norovirus Hu/GII.4/MI002/2011/USA) by 454 sequencing and compared it to the genome sequence collected from diarrhetic mouse feces 48 hpi (mouse 3 [see Table S2]) (norovirus Hu/GII.4/MI001/2011/USA) obtained by direct sequencing of PCR contigs. Only two silent nucleotide exchanges in the genome (C1576G in NS3 [NTPase] and T3058C in NS6 [protease]) were identified (data not shown), suggesting that HuNoV present in the murine feces did not undergo extensive adaptation. However, the methodologies used preclude us from determining whether the full-length genomic sequence determined from the feces of the diarrhetic mouse represents input or replicated virus.

Rag$^{-/-}$ $\gamma c^{-/-}$ mice are susceptible to infection by the intraperitoneal route. The previous studies suggested that nonhumanized BALB/c Rag$^{-/-}$ $\gamma c^{-/-}$ mice could be infected with GII.4 HuNoV following a combined intraperitoneal and oral challenge. Therefore, each route was tested individually. Eight BALB/c Rag$^{-/-}$ $\gamma c^{-/-}$ mice were infected orally with 0.05 ml GII mix containing 2.80×10^5 GII genome copies for 24 or 48 hpi, while 13 mice were infected intraperitoneally with 0.2 ml GII mix containing $1.11 \times 10e5 - 4.63 \times 10^6$ GII genome copies. Tissues and feces were collected and analyzed as described above (Fig. 2; see also Fig. S1 in the supplemental material).

In the orally inoculated mice, no genomes were detectable in any of the regions of the intestine and extraintestinal sites (see Fig. S1A in the supplemental material). Five of eight mice had detectable GII genomes in their feces during the first 24 h of infection, while no genomes were detectable prior to and between 24 and 48 hpi (see Fig. S1B in the supplemental material), suggesting

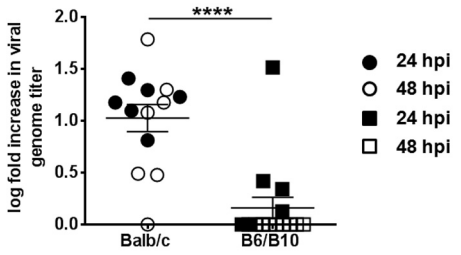

FIG 3 Susceptibility of Rag$^{-/-}$ γc$^{-/-}$ mice to HuNoV is determined in part by the genetic background of the host. Rag$^{-/-}$ γc$^{-/-}$ mice on a BALB/c or mixed C57BL/6J × C57BL/10SgSnAi background were infected intraperitoneally with HuNoV GII mix. HuNoV genomes measured in mice at 24 (filled symbols) or 48 hpi (open symbols) were compared to the inoculum to determine the log fold increase in viral genomes over input. Data are from at least three independent experiments. The mean ± SEM is indicated for each data set. Data were analyzed using the Mann-Whitney U test. ****, $P < 0.0001$.

that the detected genome was from input virus. No increases in viral loads over input were measured (data not shown). These data indicate that nonhumanized BALB/c Rag$^{-/-}$ γc$^{-/-}$ mice were not infected orally.

All 13 mice infected intraperitoneally had detectable genome titers in tissues at 24 or 48 hpi (Fig. 2). Viral genomes were detected in the intestine and extraintestinal sites, except in the brain. However, no virus was detected in the feces, suggesting that BALB/c Rag$^{-/-}$ γc$^{-/-}$ mice do not shed virus following intraperitoneal infection (Fig. 2). Overall, 12 of the 13 mice had 3- to 60-fold increases in combined genome titers in the tissues compared to the inoculum titer (Fig. 3). As a control, two mice were infected intraperitoneally with 0.2 ml GII mix containing 1.32 × 10e5 GII genome copies for 3 h, a time point prior to replication, and analyzed as before. No increases in genome titer over input were detected, suggesting that detection of increased genome titers over input titers depends on the ability of HuNoV to replicate. These data suggest that the intraperitoneal route facilitates a subclinical GII.4 infection of BALB/c Rag$^{-/-}$ γc$^{-/-}$ mice.

Susceptibility of mice to HuNoV infection is dependent on the genetic background of the host. Commercial availability of a mouse strain susceptible to HuNoV would greatly facilitate use of this mouse model. Therefore, Rag$^{-/-}$ γc$^{-/-}$ mice on a mixed C57BL/6J × C57BL/10SgSnAi background were purchased from Taconic Farms (model no. 4111) and tested for susceptibility to HuNoV. In three independent experiments, groups of five C57BL/6J × C57BL/10SgSnAi Rag$^{-/-}$ γc$^{-/-}$ mice were infected intraperitoneally with 0.2 ml GII mix containing 6.35 × 10^5 to 1.22 × 10^6 genome copies. Tissues and murine feces were analyzed as before. Viral genomes were only detected in some tissues (stomach, jejunum/duodenum, liver, spleen, mesenteric lymph nodes, and kidney) of 4 out of 15 mice (data not shown). No genomes were detectable in the feces of any of these mice (data not shown). Only 4 of 15 Rag$^{-/-}$ γc$^{-/-}$ mice on the C57BL/6J × C57BL/10SgSnAi background showed increased tissue genome loads over input (Fig. 3). There was a highly significant difference in fold increase between Rag$^{-/-}$ γc$^{-/-}$ mice on the BALB/c background and Rag$^{-/-}$ γc$^{-/-}$ mice on the C57BL/6J × C57BL/10SgSnAi background as determined using the Mann-Whitney U test ($P < 0.0001$) (Fig. 3). These data demonstrate that Rag$^{-/-}$ γc$^{-/-}$ mice on a BALB/c background are more susceptible to HuNoV infection and suggest that genetic factors of the host are important mediators of susceptibility.

Cells with macrophage-like morphology stain positive for HuNoV nonstructural and structural proteins. To confirm HuNoV replication and investigate the cell tropism of HuNoV, immunohistochemistry was performed on sections of the small intestine, spleen, and liver from BALB/c Rag$^{-/-}$ γc$^{-/-}$ mice infected intraperitoneally with GII mix for 24 and 48 h, shown in Fig. 3. To detect the viral capsid protein VP1, a polyclonal rabbit serum raised against virus-like particles (VLPs) from GII.7 HuNoV was used, since intragenogroup cross-reactive antibodies develop following VLP immunization (21). Rabbit antibodies were also raised against conserved antigenic peptide sequences in NS4 and NS6 from GII.4 strains (including KC631814 and KC631815 described herein). Preimmune sera and staining of tissue sections from mock-infected animals were used as controls.

Translation of nonstructural proteins from genomic RNA is a hallmark of (+)-sense RNA virus replication and has been used by others to demonstrate HuNoV replication in an animal model (8). In the case of BALB/c Rag$^{-/-}$ γc$^{-/-}$ mice, HuNoV NS4- and NS6-positive cells with macrophage-like morphology were observed in the splenic white pulp at the margins of the periarteriolar lymphocyte sheath spleen and in Kupffer cells of infected but not mock-infected mice (Fig. 4A, C, E, G, I, K, M, and O). No NS4- or NS6-positive cells were detected in the intestine (data not shown). Tissue sections from HuNoV-infected or mock-infected mice probed with the respective preimmune control sera were negative, demonstrating specificity of the antisera (Fig. 4B, D, F, H, J, L, N, and P).

In addition to expression of nonstructural proteins from full-length genomes, capsid proteins are expressed from subgenomic RNAs during norovirus replication (10). Therefore, sections of intestine, spleen, and liver were also stained with HuNoV VP1 antiserum. Similar to the case with NS4 and NS6 expression, capsid-specific staining was observed in cells with macrophage-like morphology in the intestine, in the white pulp of spleen, and in Kupffer cells (Fig. 5). To determine whether detection of capsid protein in these antigen-presenting cells resulted from input or replicated virus, we infected two BALB/c Rag$^{-/-}$ γc$^{-/-}$ mice intraperitoneally with GII mix (1.32 × 10e5 genome copies) for 3 h, a time point prior to replication. Tissue sections from liver and spleen were analyzed by immunohistochemistry as before, but no staining was observed (data not shown). These data indicate that capsid protein from incoming virions cannot be detected by this staining protocol, providing indirect evidence for virus replication, which results in generation of subgenomic RNA and translation of capsid proteins.

Murine NoV (MNV) is a highly prevalent pathogen in biomedical research colonies (22). Although RAG$^{-/-}$ γc$^{-/-}$ mice in our colony repeatedly tested negative by qRT-PCR for MNV (data not shown), we nevertheless directly examined the potential of the HuNoV antibodies to cross-react with MNV (see Fig. S2 in the supplemental material). Two RAG$^{-/-}$ γc$^{-/-}$ mice were infected with 1.5 × 10^5 PFU of MNV-1.CW3 by the intraperitoneal (i.p.) route for 24 h. MNV-1 titers in the spleen were 1.1 × 10^4 PFU/ml (or 5.04 × 10^7 genome copies/spleen), and titers in the liver were 3.6 × 10^3 PFU/ml (or 3.28 × 10^7 genome copies/liver). Immunohistochemistry analysis of liver and spleen sections with anti-HuNoV VP1, -NS4, and -NS6 antibodies revealed no cross-reactivity with MNV antigens (see Fig. S2A to C and E to G in the supplemental material). As a positive control, liver and spleen sections were stained with an anti-MNV VP1 antiserum, and

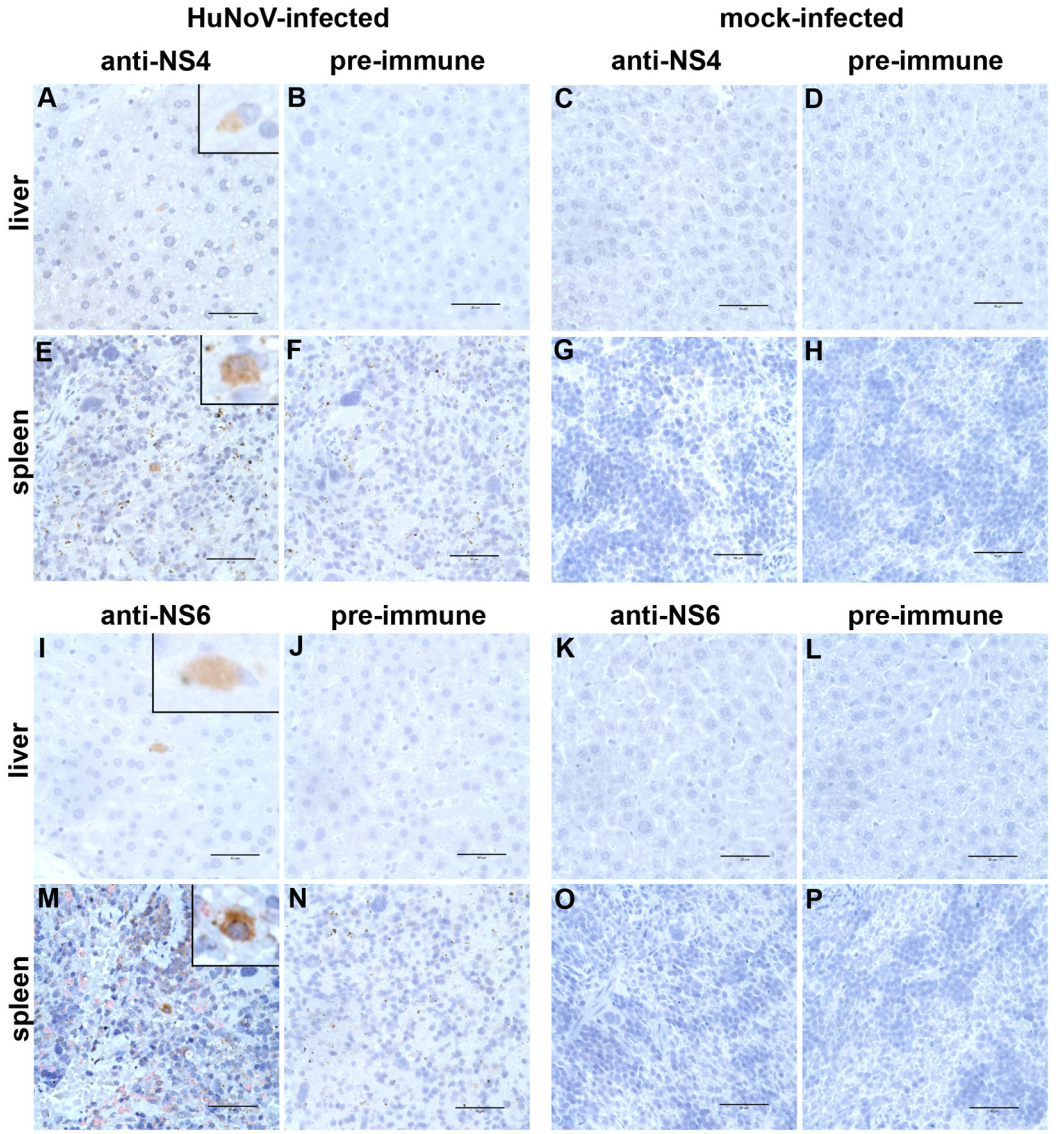

FIG 4 HuNoV nonstructural antigen staining in macrophage-like cells. Immunohistochemistry was performed with sections of spleen (E to H and M to P) or liver (A to D and I to L) using anti-NS4-specific (A, C, E, and G) or anti-NS6-specific (I, K, M, and O) immune or the respective preimmune sera (NS4 preimmune [B, D, F, and H] or NS6 preimmune [J, L, N, and P]) from Rag$^{-/-}$ γc$^{-/-}$ mice infected intraperitoneally with GII mix (A, B, E, F, I, J, M, and N) or mock stool (C, D, G, H, K, L, O, and P) for 24 h. Magnified antigen-positive cells are shown in picture insets. Scale bar = 50 μm.

MNV antigens were detected in Kupffer cells in the liver and macrophage-like cells in the spleen (Fig. S2D and H in the supplemental material), similar to our previous findings (23). Taken together, these data demonstrate that the HuNoV antisera did not cross-react with MNV antigens.

Overall, the numbers and patterns of HuNoV NS4-, NS6-, and VP1-positive cells in liver and spleen tissue were the same as those observed with anti-MNV VP1-stained liver and spleen sections and revealed a low number of individual antigen-positive cells scattered throughout the tissue (Fig. 4; see also Fig. S2 in the supplemental material; data not shown). While the low number of antigen-positive cells is likely driven by the low sensitivity of the immunohistochemistry assay, the pattern of scattered, individual antigen-positive cells of hematopoietic origin is also seen in other enteric calicivirus infections (7, 24, 25).

Histopathological analysis of hematoxylin-and-eosin-stained sections from liver, spleen, kidney, and small intestine of HuNoV-infected mice did not reveal significant changes compared to findings for mock-infected animals (data not shown), similar to findings in gnotobiotic pigs infected with HuNoV (8).

Taken together, these data provide evidence for expression of nonstructural proteins from genomic RNAs and capsid protein from subgenomic RNAs, strongly suggesting that HuNoV replicates in cells of the macrophage lineage in BALB/c Rag$^{-/-}$ γc$^{-/-}$ mice.

DISCUSSION

Study of HuNoV biology and development of antiviral therapies is hampered by the lack of a small-animal model. To overcome this limitation, the goal of these studies was to develop a HuNoV

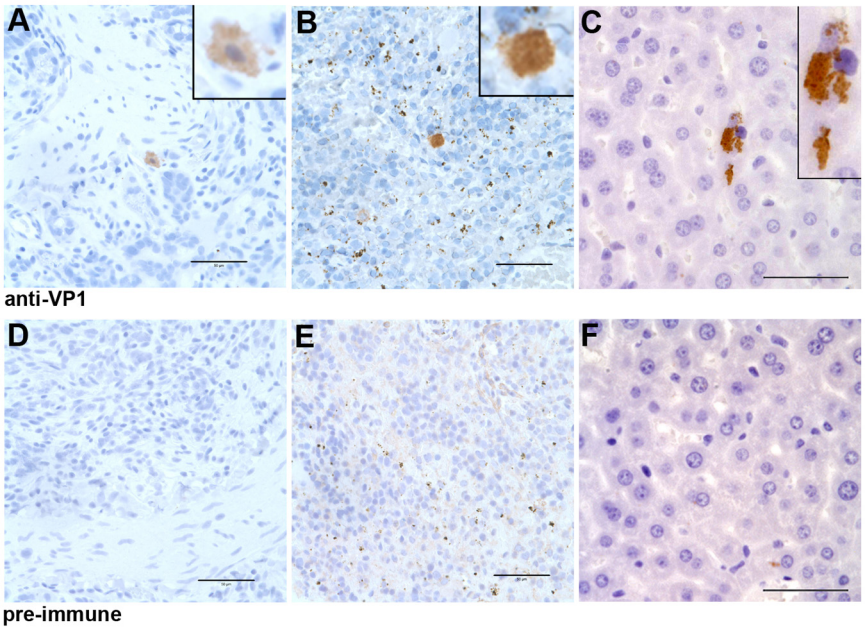

FIG 5 HuNoV capsid protein staining in macrophage-like cells. Immunohistochemistry was performed on sections of small intestine (A and D), spleen (B and E), and liver (C and F) using anti-HuNoV VP1-specific immune (A to C) and preimmune (D to F) sera from $Rag^{-/-}$ $\gamma c^{-/-}$ mice infected intraperitoneally with GII mix for 24 (A, B, D, and E) or 48 (C and F) h. Magnified antigen-positive cells are shown in picture insets. Scale bar = 50 μm.

mouse model. Our data demonstrate that humanized and nonhumanized $Rag^{-/-}$ $\gamma c^{-/-}$ mice on a BALB/c background were susceptible to a subclinical infection with HuNoV as indicated by detection of nonstructural protein-positive cells and capsid-positive cells, as well as increases in genome titers over input.

First, expression of nonstructural proteins, which are expressed only during infection (10), has been used in the case of HuNoV infection of gnotobiotic pigs (8) as one line of evidence to demonstrate HuNoV replication. Similarly, our data show that two independent antibodies directed against two nonstructural proteins detected antigen-positive cells in infected but not mock-infected mice (Fig. 4). Furthermore, the corresponding preimmune sera did not react with any antigens, and no cross-reactivity with the related MNV nonstructural proteins was observed.

Second, subgenomic RNAs are made during replication to express the noroviral capsid protein (10). Thus, detection of capsid protein at levels greater than those of incoming capsids is additional evidence for HuNoV replication and was used in several other HuNoV animal models (7, 8, 9). We detected capsid protein expression in livers and spleens of mice infected intraperitoneally with HuNoV for 24 h but failed to detect capsid-positive cells in the livers and spleens of mice infected for 3 h (Fig. 5 and data not shown). This demonstrated that capsid protein from input virus cannot be detected by immunohistochemistry and suggested that the capsid protein detected at 24 hpi was translated from newly synthesized viral subgenomic RNA. The number and pattern of HuNoV nonstructural protein-positive cells in liver and spleen tissue was similar to that observed using an antibody against the HuNoV capsid protein (Fig. 4 and 5), suggesting that translation of nonstructural proteins, subgenomic replication, and translation of the capsid protein occurred in a single cell.

Third, increases in overall genome titers over input were used as another independent piece of evidence of replication. Up to 1,400-fold increases over input were detected in genome titers in mice infected by a combined oral/intraperitoneal administration, and up to 60-fold increases were detected in mice infected intraperitoneally. The significant increases in genome titers over input were observed in two independent laboratories. Moreover, the likelihood that merely input virus in tissue samples was detected is low because no increases over input virus were observed in multiple experiments in which mice were inoculated with HuNoV, e.g., combined oral/intraperitoneal infection of wild-type BALB/c mice (Fig. 1C), oral infection of $Rag^{-/-}$ $\gamma c^{-/-}$ mice (see Fig. S2 in the supplemental material), and intraperitoneal infection of $Rag^{-/-}$ $\gamma c^{-/-}$ mice for 3 h, a time point prior to replication (data not shown).

Our data further demonstrated that $Rag^{-/-}$ $\gamma c^{-/-}$ mice reconstituted with CD34-positive human stem cells showed no statistically significant difference from nonhumanized mice. Thus, susceptibility was not linked to human cell reconstitution in this mouse model, and this suggested that HuNoV may replicate in cells of murine origin. Immunohistochemistry of infected tissues showed HuNoV capsid-, NS4-, and NS6-positive Kupffer cells and macrophage-like cells in the spleen (Fig. 4 and 5). This is similar to murine norovirus (MNV), where antigen-positive Kupffer cells in the liver and splenic cells with macrophage-like morphology were observed (23, 26) (see Fig. S2 in the supplemental material). A tropism of HuNoV for macrophages, a cell type present in the intestinal lamina propria, is also consistent with the previous finding that HuNoV GII.4 virus-like particles bind to lamina propria cells of human duodenum tissue sections (16). Thus, HuNoV and MNV may share a tropism for cells of the hematopoietic lineage. The identification of a cell type from the murine host, which supports HuNoV infection, may lead to the development of a HuNoV tissue culture system in the future.

We also demonstrated that $Rag^{-/-}$ $\gamma c^{-/-}$ mice on a C57BL/6J

× C57BL/10SgSnAi background were less susceptible to HuNoV than Rag$^{-/-}$ γc$^{-/-}$ mice on a BALB/c background. Therefore, susceptibility may depend on the genetic background and/or immune deficiencies. Differences in susceptibility due to genetic backgrounds are also observed with other pathogens, and an increased susceptibility of BALB/c mice compared to that of C57BL6 or C57BL10 mice due to differences in the host immune response has been described (e.g., see references 27 to 29). For example, production of type I interferons by peritoneal macrophages/monocytes was significantly increased in C57BL6 mice over that in BALB/c mice (27). HuNoV replication is sensitive to type I interferons (30, 31). Thus, HuNoV injected intraperitoneally in C57BL/6J × C57BL/10SgSnAi mice potentially encounters higher levels of type I interferons, which in turn could limit virus infection. Further studies will be required to identify host factors determining HuNoV susceptibility in this mouse model.

Interestingly, our study suggests that Rag$^{-/-}$ γc$^{-/-}$ mice are not susceptible to oral infection. This is in contrast to HuNoV transmission in humans, which occurs via the fecal-oral route, and in gnotobiotic pigs, which are permissive to HuNoV following oral infection (31). This lack of oral infection in Rag$^{-/-}$ γc$^{-/-}$ mice may be due to the genetic deficiency in the common cytokine receptor gamma chain (γc) in these mice. Several enteric pathogens use specialized microfold (M) cells present in the follicle-associated epithelium overlaying Peyer's patches to gain access to their host (for review, see reference 32). However, Peyer's patches were absent from Rag$^{-/-}$ γc$^{-/-}$ mice following macroscopic and histological observation (data not shown). This is not surprising, since signaling through the interleukin 7 (IL-7) receptor, which is a heterodimer comprised of the IL-7 alpha chain and common gamma chain, is critical for Peyer's patch development (33, 34). We hypothesize that a lack of M cells may prevent oral HuNoV infection in this mouse model, and studies are currently under way to test this hypothesis.

In addition, we did not observe HuNoV genome in the feces of mice following intraperitoneal infection alone at any of the analyzed time points. In contrast, viral genomes were detected in the feces of mice infected both intraperitoneally and orally or orally only. HuNoV genome titers in murine feces were less than input levels following oral infection, suggesting that the viral genomes detected represent input virus. Genome titers in murine feces greater than that of input virus were detected when mice were infected by combined intraperitoneal and oral inoculation. Future studies are needed to determine the relative amounts of replicated virus shed under these conditions. In addition, our finding raises a broader unanswered question in norovirus pathogenesis, which is how noroviruses are shed from their host. Rag$^{-/-}$ γc$^{-/-}$ mice may provide an important tool to address this question in the future.

In summary, Rag$^{-/-}$ γc$^{-/-}$ mice on a BALB/c background are susceptible to a subclinical infection by HuNoV, providing the first small-animal model for HuNoV infection. While this mouse model does not recapitulate all aspects of HuNoV infection, such as fecal-oral transmission, it will allow further mechanistic studies of HuNoV biology, including host and viral factors determining susceptibility, which might enable improvement of the mouse model. Furthermore, it is our hope that the availability of an easily manipulable small-animal model for HuNoV infection will facilitate not only basic but also translational HuNoV research, such as efficacy testing of compounds with anti-HuNoV activity, thereby accelerating the development of urgently needed HuNoV therapeutics.

MATERIALS AND METHODS

Detailed methods can be found in Text S1 in the supplemental material.

HuNoV samples. Ten human stool samples from confirmed HuNoV outbreaks (see Table S1 in the supplemental material) were processed as outlined in Text S1.

Mice. All animal studies described herein were performed in accordance with local and federal guidelines. Please refer to Text S1 in the supplemental material for details.

Infection of mice. Mice were housed individually in wire-bottom cages, and murine feces were collected over the indicated time frames. Mice were infected and harvested as outlined in Text S1.

Quantification/typing of HuNoV genomes by qRT-PCR. Quantitative RT-PCR of the HuNoV genome was performed with total RNA from fecal and tissue samples as detailed in Text S1 in the supplemental material. The sensitivity and specificity of the assay are outlined in Text S1. Fecal samples were subjected to genotyping as detailed in Text S1.

Determination of fold increase. Inoculum titers were determined for each experiment after back titration of the human stool suspensions by qRT-PCR. Total genome copies per mouse were calculated by adding genome copies in all tissues and feces as outlined in Text S1 in the supplemental material. The fold change was determined by dividing total genome copies by inoculum genome copies.

Sequencing. Total nucleic acid was isolated from 0.2 ml of clarified human stool filtrate of patients 9 and 10 (see Table S1 in the supplemental material), and 454 pyrosequencing was performed. A genome sequence of HuNoV GII was obtained from mouse feces 48 h postinfection using Sanger sequencing of PCR amplicons (GenBank no. KC631815) (see Text S1 for additional details).

Generation of antibodies. Anti-VLP antibodies were made at Cocalico Biologicals, Inc., Reamstown, PA, in rabbits, following standard protocols. Nonstructural antibodies against conserved antigenic NS4 and NS6 peptide sequences were generated and were affinity purified at GenScript USA Inc., Piscataway, NJ, in rabbits, following standard protocols. Preimmune sera were collected from each rabbit used to generate each antibody (see Text S1 in the supplemental material for additional details).

Histopathology and immunohistochemistry. Mouse tissues were fixed and processed at the University of Michigan Pathology Core for Animal Research, following standard histological procedures (see Text S1 in the supplemental material for additional details).

Statistical analysis. The software program GraphPad Prism V5 (GraphPad, La Jolla, CA) was used to perform statistical analyses. The Mann-Whitney U test was used to analyze differences. Results were considered statistically significant when the P value was <0.05.

Nucleotide sequence accession numbers. The genomic sequences for the HuNoV GII strain obtained from feces of the mouse with diarrhea (norovirus Hu/GII.4/MI001/2011/USA; accession number KC631814), the original inoculum (norovirus Hu/GII.4/MI002/2011/USA; accession number KC631815), and the GII.7 HuNoV used for VLP production (accession number KC832474) have been deposited in GenBank.

SUPPLEMENTAL MATERIAL

Supplemental material for this article may be found at http://mbio.asm.org/lookup/suppl/doi:10.1128/mBio.00450-13/-/DCSupplemental.

Text S1, DOCX file, 0.1 MB.
Figure S1, TIF file, 1.1 MB.
Figure S2, TIF file, 6.5 MB.
Table S1, XLSX file, 0.1 MB.
Table S2, XLSX file, 0.1 MB.

ACKNOWLEDGMENTS

This work was supported by NIH grants AI080611 to C.E.W. and AI073255 to R.A. S.A.H. and L.B.T. were supported by NIH grants AI0544483, U54 AI057160, and AI084887.

We thank the University of Michigan Pathology Core for Animal Research for excellent technical assistance, I. Weissman (Stanford University) for Rag$^{-/-}$ $\gamma c^{-/-}$ mice, the Michigan Department of Community Health for HuNoV-containing human stool samples, and M. J. Gonzalez-Hernandez (University of Michigan) for critical reading of the manuscript.

REFERENCES

1. **Widdowson MA, Monroe SS, Glass RI.** 2005. Are noroviruses emerging? Emerg. Infect. Dis. **11:**735–737.
2. **Patel MM, Widdowson MA, Glass RI, Akazawa K, Vinjé J, Parashar UD.** 2008. Systematic literature review of role of noroviruses in sporadic gastroenteritis. Emerg. Infect. Dis. **14:**1224–1231.
3. **Hall AJ, Curns AT, McDonald LC, Parashar UD, Lopman BA.** 2012. The roles of Clostridium difficile and norovirus among gastroenteritis-associated deaths in the United States, 1999–2007. Clin. Infect. Dis. **55:** 216–223.
4. **Scallan E, Hoekstra RM, Angulo FJ, Tauxe RV, Widdowson MA, Roy SL, Jones JL, Griffin PM.** 2011. Foodborne illness acquired in the United States—major pathogens. Emerg. Infect. Dis. **17:**7–15.
5. **Atmar RL, Estes MK.** 2006. The epidemiologic and clinical importance of norovirus infection. Gastroenterol. Clin. North Am. **35:**275–290.
6. **Scharff RL.** 2010. Health related costs from foodborne illness in the United States. Georgetown University, Washington, DC.
7. **Bok K, Parra GI, Mitra T, Abente E, Shaver CK, Boon D, Engle R, Yu C, Kapikian AZ, Sosnovtsev SV, Purcell RH, Green KY.** 2011. Chimpanzees as an animal model for human norovirus infection and vaccine development. Proc. Natl. Acad. Sci. U. S. A. **108:**325–330.
8. **Cheetham S, Souza M, Meulia T, Grimes S, Han MG, Saif LJ.** 2006. Pathogenesis of a genogroup II human norovirus in gnotobiotic pigs. J. Virol. **80:**10372–10381.
9. **Souza M, Azevedo MS, Jung K, Cheetham S, Saif LJ.** 2008. Pathogenesis and immune responses in gnotobiotic calves after infection with the genogroup II.4-HS66 strain of human norovirus. J. Virol. **82:**1777–1786.
10. **Green KY.** 2007. Caliciviridae, p 949–980. *In* Knipe DM, Howley PM (ed), Fields Virology, vol **1**, 5th ed. Lippincott Williams & Wilkins, Philadelphia, PA.
11. **Zheng DP, Ando T, Fankhauser RL, Beard RS, Glass RI, Monroe SS.** 2006. Norovirus classification and proposed strain nomenclature. Virology **346:**312–323.
12. **Bull RA, Eden JS, Rawlinson WD, White PA.** 2010. Rapid evolution of pandemic noroviruses of the GII.4 lineage. PLoS Pathog. **6:**e1000831. http://dx.doi.org/doi:10.1371/journal.ppat.1000831.
13. **Bull RA, White PA.** 2011. Mechanisms of GII.4 norovirus evolution. Trends Microbiol. **19:**233–240.
14. **CDC.** 2013. Notes from the field: emergence of new norovirus strain GII.4 Sydney—United States, 2012. MMWR Morb. Mortal. Wkly. Rep. **62:**55.
15. **Vinjé J.** 2010. A norovirus vaccine on the horizon? J. Infect. Dis. **202:** 1623–1625.
16. **Chan MC, Ho WS, Sung JJ.** 2011. In vitro whole-virus binding of a norovirus genogroup II genotype 4 strain to cells of the lamina propria and Brunner's glands in the human duodenum. J. Virol. **85:**8427–8430.
17. **Akkina R, Berges BK, Palmer BE, Remling L, Neff CP, Kuruvilla J, Connick E, Folkvord J, Gagliardi K, Kassu A, Akkina SR.** 2011. Humanized Rag1-/-gammac-/- mice support multilineage hematopoiesis and are susceptible to HIV-1 infection via systemic and vaginal routes. PLoS One **6:**e20169. doi: 10.1371/journal.pone.0020169.
18. **Hoehne M, Schreier E.** 2006. Detection of norovirus genogroup I and II by multiplex real-time RT-PCR using a 3′-minor groove binder-DNA probe. BMC Infect. Dis. **6:**69. doi: 10.1186/1471-2334-6-69.
19. **Matthews JE, Dickey BW, Miller RD, Felzer JR, Dawson BP, Lee AS, Rocks JJ, Kiel J, Montes JS, Moe CL, Eisenberg JN, Leon JS.** 2012. The epidemiology of published norovirus outbreaks: a review of risk factors associated with attack rate and genogroup. Epidemiol. Infect. **140:** 1161–1172.
20. **Zaini Z, Phuektes P, McMinn P.** 2012. Mouse adaptation of a subgenogroup B5 strain of human enterovirus 71 is associated with a novel lysine to glutamic acid substitution at position 244 in protein VP1. Virus Res. **167:**86–96.
21. **Parker TD, Kitamoto N, Tanaka T, Hutson AM, Estes MK.** 2005. Identification of genogroup I and genogroup II broadly reactive epitopes on the norovirus capsid. J. Virol. **79:**7402–7409.
22. **Henderson KS.** 2008. Murine norovirus, a recently discovered and highly prevalent viral agent of mice. Lab. Anim. (NY) **37:**314–320.
23. **Wobus CE, Karst SM, Thackray LB, Chang KO, Sosnovtsev SV, Belliot G, Krug A, Mackenzie JM, Green KY, Virgin HW.** 2004. Replication of norovirus in cell culture reveals a tropism for dendritic cells and macrophages. PLoS Biol. **2:**e432. doi: 10.1371/journal.pbio.0020432.
24. **Mumphrey SM, Changotra H, Moore TN, Heimann-Nichols ER, Wobus CE, Reilly MJ, Moghadamfalahi M, Shukla D, Karst SM.** 2007. Murine norovirus 1 infection is associated with histopathological changes in immunocompetent hosts, but clinical disease is prevented by STAT1-dependent interferon responses. J. Virol. **81:**3251–3263.
25. **Sestak K, Feely S, Fey B, Dufour J, Hargitt E, Alvarez X, Pahar B, Gregoricus N, Vinjé J, Farkas T.** 2012. Experimental inoculation of juvenile rhesus macaques with primate enteric caliciviruses. PLoS One **7:**e37973. doi: 10.1371/journal.pone.0037973.
26. **Ward JM, Wobus CE, Thackray LB, Erexson CR, Faucette LJ, Belliot G, Barron EL, Sosnovtsev SV, Green KY.** 2006. Pathology of immunodeficient mice with naturally occurring murine norovirus infection. Toxicol. Pathol. **34:**708–715.
27. **Ellermann-Eriksen S, Liberto MC, Iannello D, Mogensen SC.** 1986. X-linkage of the early in vitro alpha/beta interferon response of mouse peritoneal macrophages to herpes simplex virus type 2. J. Gen. Virol. **67:** 1025–1033.
28. **Geist LJ, Hinde SL.** 2001. Susceptibility to cytomegalovirus infection may be dependent on the cytokine response to the virus. J. Investig. Med. **49:**434–441.
29. **Güler ML, Gorham JD, Hsieh CS, Mackey AJ, Steen RG, Dietrich WF, Murphy KM.** 1996. Genetic susceptibility to Leishmania: IL-12 responsiveness in TH1 cell development. Science **271:**984–987.
30. **Chang KO, George DW.** 2007. Interferons and ribavirin effectively inhibit Norwalk virus replication in replicon-bearing cells. J. Virol. **81:** 12111–12118.
31. **Jung K, Wang Q, Kim Y, Scheuer K, Zhang Z, Shen Q, Chang KO, Saif LJ.** 2012. The effects of simvastatin or interferon-alpha on infectivity of human norovirus using a gnotobiotic pig model for the study of antivirals. PLoS One **7:**e41619. doi: 10.1371/journal.pone.0041619.
32. **Miller H, Zhang J, Kuolee R, Patel GB, Chen W.** 2007. Intestinal M cells: the fallible sentinels? World J. Gastroenterol. **13:**1477–1486.
33. **Honda K, Nakano H, Yoshida H, Nishikawa S, Rennert P, Ikuta K, Tamechika M, Yamaguchi K, Fukumoto T, Chiba T, Nishikawa SI.** 2001. Molecular basis for hematopoietic/mesenchymal interaction during initiation of Peyer's patch organogenesis. J. Exp. Med. **193:**621–630.
34. **Luther SA, Ansel KM, Cyster JG.** 2003. Overlapping roles of CXCL13, interleukin 7 receptor alpha, and CCR7 ligands in lymph node development. J. Exp. Med. **197:**1191–1198.
35. **Berges BK, Wheat WH, Palmer BE, Connick E, Akkina R.** 2006. HIV-1 infection and CD4 T cell depletion in the humanized Rag2-/-gamma c-/- (RAG-hu) mouse model. Retrovirology **3:**76. doi: 10.1186/1742-4690-3-S1-S76.